SLAS Technology xxx (xxxx) xxx

Contents lists available at ScienceDirect

SLAS Technology

journal homepage: www.elsevier.com/locate/slast

Technologies bringing young Zebrafish from a niche field to the limelight

Jason J Otterstrom[a], Alexandra Lubin[b], Elspeth M Payne[b,*], Yael Paran[a,*]

[a] IDEA Bio-Medical Ltd., Rehovot, Israel
[b] Research Department of Hematology, Cancer Institute, University College London, London, UK

ARTICLE INFO

Keywords:
Zebrafish
High-Content Screening
Automation
Artificial Intelligence
Image Analysis

ABSTRACT

Fundamental life science and pharmaceutical research are continually striving to provide physiologically relevant context for their biological studies. Zebrafish present an opportunity for high-content screening (HCS) to bring a true in vivo model system to screening studies. Zebrafish embryos and young larvae are an economical, human-relevant model organism that are amenable to both genetic engineering and modification, and direct inspection via microscopy. The use of these organisms entails unique challenges that new technologies are overcoming, including artificial intelligence (AI).

In this perspective article, we describe the state-of-the-art in terms of automated sample handling, imaging, and data analysis with zebrafish during early developmental stages. We highlight advances in orienting the embryos, including the use of robots, microfluidics, and creative multi-well plate solutions. Analyzing the micrographs in a fast, reliable fashion that maintains the anatomical context of the fluorescently labeled cells is a crucial step. Existing software solutions range from AI-driven commercial solutions to bespoke analysis algorithms. Deep learning appears to be a critical tool that researchers are only beginning to apply, but already facilitates many automated steps in the experimental workflow. Currently, such work has permitted the cellular quantification of multiple cell types in vivo, including stem cell responses to stress and drugs, neuronal myelination and macrophage behavior during inflammation and infection. We evaluate pro and cons of proprietary versus open-source methodologies for combining technologies into fully automated workflows of zebrafish studies. Zebrafish are poised to charge into HCS with ever-greater presence, bringing a new level of physiological context.

Background

High-content screening (HCS) is a microscopy-based research workflow that automates data acquisition for a phenotypic assay [1]. It enables the use of multiple experimental conditions in parallel to extract detailed information from large numbers of samples and performs imaging and analysis in an unbiased fashion. Fields such as cancer [2,3], Infectious disease [4] and drug discovery [5,6], have high demand for HCS approaches, which traditionally acquire data from 2D cell culture [1,7]. Increasing demands from researchers for more physiologically relevant biological systems are bringing in new models to the field of HCS [7,8]. Zebrafish are one such model system of interest [9].

Automated sample preparation technologies achieve the highest throughput in HCS, such as liquid handlers and robotic plate manipulators [1]. Samples are then visualized using a computer-controlled microscope that substitutes a human worker in obtaining digital, microscopic images of a specimen. Through these HCS technologies, sophisticated preparation and image acquisition workflows can be performed in a fully autonomous fashion.

A second step in HCS is computer-controlled analysis of the resulting images to quantify metrics that inform researchers of phenotypic changes to experimental conditions [1,10,11]. Such automation enables unbiased data collection and analysis. It also provides traceability and reproducibility of the experimental workflow since computers record and document every step. Such approaches are common in the field of drug discovery and are most advanced in relation to imaging of single cells in 2D culture conditions.

A key element of the HCS approach is the ability to not only detect and measure primary objects of interest, but also identify secondary objects within the primary objects [1,10], such as spots or nuclear bodies. For instance, with reference to 2D cell culture, identifying a cell border along with its internal nucleus and organelles or other structure. Thus, analysis must integrate and utilize as much information as possible to maximize benefit from technology investment. Such approaches provide a wealth of information regarding the underlying phenotype, as highlighted in Figure 1.

Demand is increasing for replicating in vivo biological models in the HCS field in general and specifically within drug discovery [7]. This re-

HCS, High-Content Screening; AI, Artificial Intelligence; hpf, hours post fertilization; dpf, days post fertilization.

* Corresponding authors.

https://doi.org/10.1016/j.slast.2021.12.005

Available online xxx

Please cite this article as: J.J. Otterstrom, A. Lubin, E.M. Payne et al., Technologies bringing young Zebrafish from a niche field to the limelight, SLAS Technology, https://doi.org/10.1016/j.slast.2021.12.005

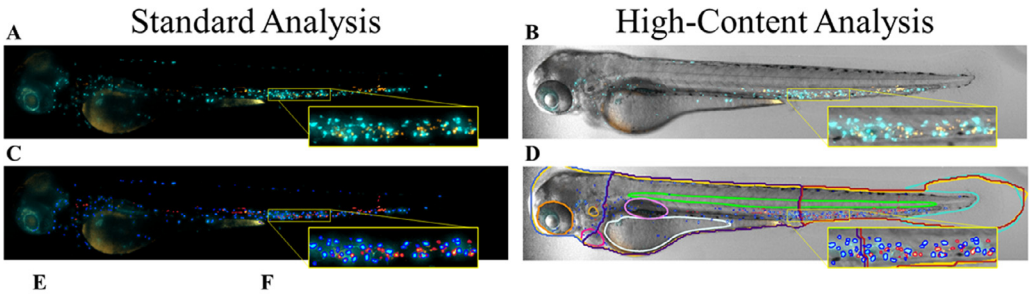

E

Spot Count	Total
CD41-GFP	193
Lysc-mCherry	339

F

Spot Count	Fish	Yolk	Eye	Fin	Noto-cord	Otic Vesicle	Swim Bladder	Heart	Head	Trunk	Tail
CD41-GFP	193	0	2	0	1	1	2	0	23	74	95
Lysc-mCherry	339	14	6	0	1	1	14	3	39	182	118
Anatomic Area [mm^2]	1.3	0.14	0.05	0.22	0.10	0.003	0.035	0.016	0.25	0.61	0.45

Fig. 1. High-Content Analysis vs. Standard Analysis. **A)** Image showing fluorescence channels of a 4 dpf zebrafish embryo labeled with CD41:GFP [26] (orange) and lysC:mCherry [27] (cyan) to visualize hematopoietic stem cells and thrombocytes, and myeloid cells, respectively. Zoom-in highlights the cell types visible in the tail region. **B)** Brightfield and fluorescence channel overlay of the image in (A). **C)** Image from (A) with CD41:GFP and lysC:mCherry expressing cells identified by fluorescence image analysis to permit counting of cells or cell clusters. **D)** Image from (B) with zebrafish anatomy identified through automatic AI based image analysis [28] to group the identified cells/cell clusters found through fluorescence image analysis. **E)** Quantification of cell/cluster counting in the two fluorescence channels from panel (C). **F)** Quantification as in (E), but with each cell/cluster associated with the relevant zebrafish anatomy identified in (D), which also quantifies area of anatomical structures. *Outline colors:* Fish contour (yellow), head (blue), trunk (dark purple), tail (dark red), eye (orange), heart (dark pink), otic vesicle (golden), yolk sac (white), swim bladder (light pink), notochord (light green), tail fin (light blue), CD41:GFP (red spot outlines), lysC:mCherry (dark blue spot outlines).

sults from continuing high levels of compound attrition in clinical studies due to detrimental toxicological side effects [8]. In response, HCS is rapidly growing into the field of 3D cell culture, such as spheroids and organoids, and lab-on-a-chip technologies [8,12,13]. These approaches demonstrate that they improve the quality of 'hits' they identify [8].

For in vivo studies using a whole organism, zebrafish are rapidly becoming a popular choice [8], particularly for developmental [14], drug screening [15,16] and toxicology [17] studies. They benefits from economical husbandry [18], and are a fast-growing model organism whose initial development, from zygote to larvae [19,20], can be visualized under the microscope thanks to their small size and semi-transparency. These traits permit visualization of the internal anatomy of zebrafish larva using low magnification brightfield images (Figure 1), which can be obtained using many types of microscopes. Fertilized zebrafish eggs are readily identifiable, and the developing embryo is optically transparent permitting visualization of internal organs, organ systems and even single cells up to 120 hpf (hours post fertilization).

Moreover, the zebrafish model is human-relevant. Not only is it a vertebrate animal, but zebrafish also have orthologues to approximately 70% of human genes [21], thus making them attractive for studies involving genetic diseases [22], including cancer [23], and the development of therapeutics [24]. Additionally, the entire zebrafish genome is sequenced, and they are amenable to both genetic engineering and modification, for instance through CRISPR/Cas9 technology [25]. For example, the larva shown in Figure 1 is modified with both Tg(CD41:GFP) [26] and Tg(lyzC:mCherry) [27] to tag the CD41 glycoprotein with GFP to visualize hematopoietic stem cells and thrombocytes, and to express cytosolic mCherry through a *lyz* promoter to visualize myeloid cells, respectively. Hence, labeling different cell lines within the zebrafish enables specific visualization of cells of interest inside these live, transparent animals [28].

Experimental workflows for microscopy of zebrafish begin with sorting fertilized eggs. This step is a relatively quick process, requiring only 5–10 minutes for a trained technician [29]. Selected eggs develop into early embryos surrounded by a protective pouch termed the chorion until approximately 48 hpf. For best imaging conditions and for toxicology studies [30], the chorion must be removed through a process of dechorionation. For genetic and other types of studies, the embryo must also undergo microinjection. Once ready for the microscope, the embryo needs to be oriented to optimize imaging of internal anatomy. This involves placing the animal either on its side (lateral orientation) or on its back (dorsal orientation). Imaging can then be performed manually or automatically using multiple types of microscope setups.

While manual study of zebrafish is commonplace, several bottlenecks exist to automating HCS workflows and we have categorized conceptual steps in Figure 2. Relative to the imaging step, upstream bottlenecks involve sample preparation and handling, while those downstream involve automated and unbiased image analysis [12] to maximize data extraction while maintaining anatomical context.

In this perspective, we focus on adaptation of fully automated workflows to become built around zebrafish, including robotic sample manipulation and automated analysis of images akin to that shown in Figure 1. The studies described here utilize anesthetized or awake, immobilized fish, though rich and informative data, too, arise from well-developed fields studying zebrafish behavior, which we do not included. Many advances have emerged in recent years, though many opportunities exist to fill in gaps in automatization of zebrafish screening, particularly around sample manipulation.

State-of-the-art Automation

Zebrafish sample preparation and handling

Thanks to the fast zebrafish development time, many toxicology, gene regulation or knockdown studies utilizing zebrafish can give results within five days post fertilization (5 dpf). Such studies may utilize a combination of dechorionation and/or microinjection of an early-stage embryo, which currently have limited options for automation. Once an embryo has undergone any relevant manipulation, it must be prepared for imaging. Orienting the animal for microscopic image acquisition is yet an additional obstacle, but automated solutions exist and are developing to overcome this obstacle.

Embryo microinjection

Microinjection of an early-stage embryo allows insertion of fluorophores, nanoparticles, bacteria, DNA constructs, mRNA for overexpression, morpholino antisense oligonucleotides (MOs) for knockdown and CRISPR/Cas9 for gene editing. The ease of performing individual injections, and the variety of experiments it enables, makes microinjection one of the most common techniques in zebrafish research.

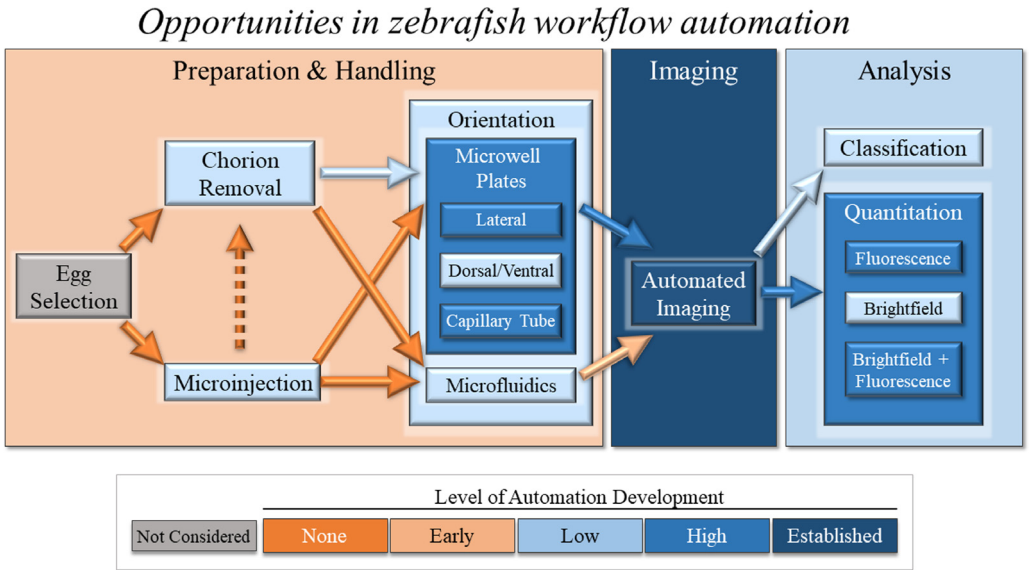

Fig. 2. Schematic of sample handling and data processing steps in a workflow for automated zebrafish embryo/larvae screening. Rectangles represent conceptual categories of steps beginning with zebrafish sample preparation and handling, followed by sample imaging, finalized by analysis of the images. Arrows represent movement of either the zebrafish samples or the extracted data between categories; solid arrows are necessary steps while dashed indicate optional ones. Each rectangle or arrow is color coded to represent a qualitative amount of existing automated technologies present either within each category (rectangle) or to move between categories (arrow). Dark orange implies that no automated technologies exist and, hence, highest need; light orange indicate basic demonstrations with ample space for innovation; light blue indicate multiple demonstrations with space only for incremental steps; dark blue indicate a high level of automation with established technologies. Egg selection, in grey, is not included in the survey.

A notable challenge arises when performing these experiments at scale. A novel approach by Cordero-Maldonado et al. [31] to automate the procedure utilized Deep Learning for image recognition. This computer vision enabled automated selection of a site for computer controlled microinjection into embryos at the one- or two-cell stage of development, building upon an approach they reported earlier [32,33].

The authors' setup involved arranging the zebrafish embryos into a grid, like the one shown in Figure 3A, containing 100 wells covered with 1% agarose. The authors tested injection of embryos with MOs, CRISPR/Cas9 and DNA constructs and investigated their efficacy. Different types of injections each have differing requirements for injection site selection, hence efficacy of one type does not necessarily extend to another. The authors performed MOs injections into the yolk, while CRISPR/Cas9 system and DNA constructs into the blastomere or yolk boundary. It can be challenging to rapidly inject into the blastomere manually, requiring additional training and technical skill. For some injections, such as RNA, the embryos required orientation with an artist paintbrush. Embryo orientation within the agarose-filled grid proved critical to maximizing efficacious microinjection, with reduced efficacy when the first cell was not visible.

Computer-controlled injection software first selected viable, single-cell embryos with an accuracy of 93%. The software then identified the injection site within 42 μm of human-annotated desirable location, on average, with an execution time of tens of milliseconds. This fast and precise operation achieved throughputs 1.5x–2x faster than manual injection for MOs or DNA construct injection, with equivalent efficacy. CRISPR/Cas9 microinjection was 3.6x faster than manual, but at the expense of lower efficacy due to non-optimal embryo orientation, giving a 1.5x higher throughput all together.

The benefit is threefold overall: higher throughput, elimination of required skill sets and freeing the time of experts to perform non-automated research. However, manual intervention is still required to maximize automated injection efficacy and expert humans can achieve the highest efficacies should they be required [31]. The authors have commercialized their solution and through Life Science Methods B.V. in the Netherlands.

Embryo Dechorionation

Zebrafish develop in a spherical protective chorion, from which they will hatch naturally at 2-3 dpf. However, zebrafish can survive outside the chorion following manual or enzymatic removal. Dechorionation is a requisite first step for some toxicology assays [30], and as a preparative step for imaging via microscopy since it allows the embryo to favorably unwrap itself and elongate. Chemical dechorionation is a fast, manual process requiring little time and without causing bottlenecks. Subsequent deposition of dechorionated embryos into sample plates, however, is a bottleneck to performing experiments at scale.

Mandrell et al. [29] automated both processes together to achieve high-throughput dechorionation of approximately 1600 zebrafish embryos and placement into a 96-well plate. The authors designed a liquid handling system built upon a mechanical shaker to agitate the embryos during Pronase protease treatment to remove the chorion. Subsequently, a machine vision-guided robotic arm holding a Pasture pipet would select suitable embryos using custom software and deposit them into the plate.

Impressively, they demonstrated >95% chorion removal from 4 hpf with only 2% mortality rate at 24 hpf and an additional 2% malformation rate at 5 dpf. The robot then dispensed dechorionated embryos into 96-well plates automatically with an accuracy of 94.7% and only 2.8% mortality rate. Altogether, ~85% of the embryos were alive when placed into the plates, dechorionated and without injury. Throughput rate achieved a substantial enhancement, processing approximately 2000 embryos/hour while the manual station achieved ~250/hour, albeit with a higher (95%) survival rate and half the number of malformations. By combining the processes together with very young embryos, the approach by Mandrell et al. [29] may enable sample preparation at the scale needed for HCS.

Embryo orientation

Once the embryos are dechorionated, they can be placed into multi-well plates for imaging. Proper orientation of the fish either on their side, ventrally, or on their back, dorsally, is often necessary to obtain proper visualization of certain anatomical structures or regions under the microscope. Two technologies highlighted here are side-orienting

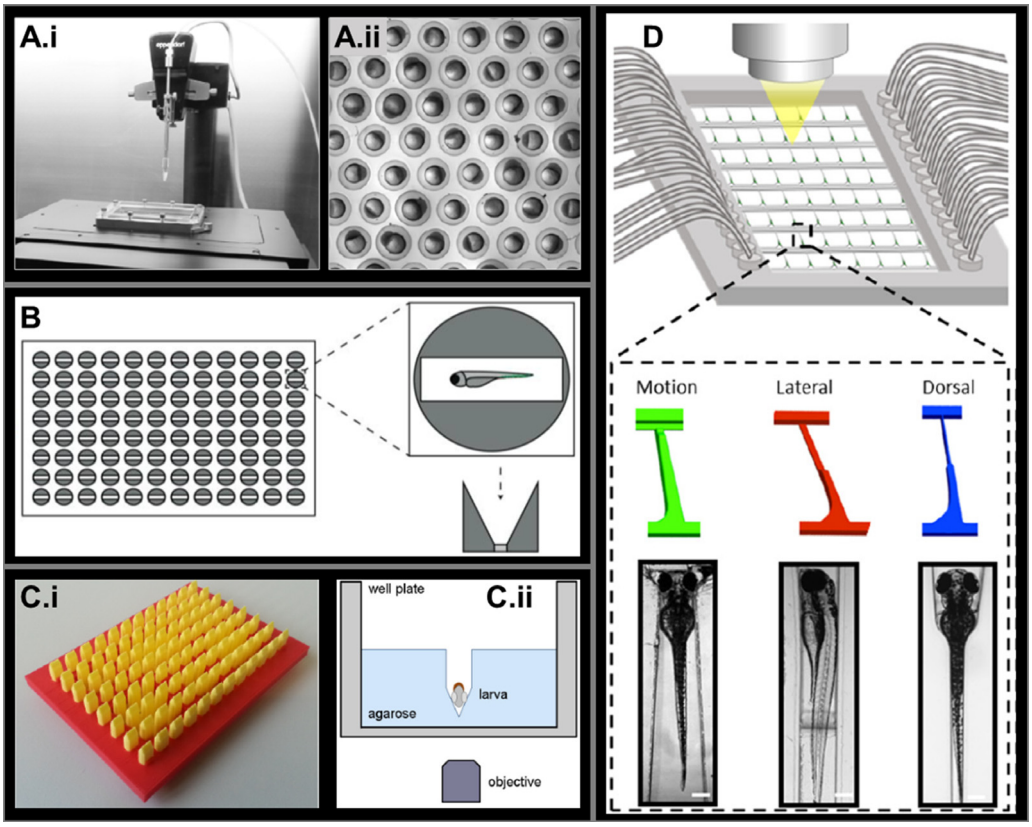

Fig. 3. Technologies for automated microinjection and orientation control of zebrafish embryos or larvae. A) Automated microinjection. (i) Photograph of a zebrafish embryo microinjection robot placed inside a laminar flow cabinet. Life Science Methods B.V. distributes a similar robot that is driven by a computer vision system using a deep-learning algorithm for injection site identification within embryos [31]; (ii) grid of embryos held in place by agarose. Both (i) and (ii) are reprinted from Carvalho et al. [32] under CC-BY license; original photographs have been cropped to fit. B) Illustration of the Hashimoto zebrafish orienting 96-well plate. The zoom-in depicts the rectangular visualization window. Below the zoom-in, the steeply inclined sides of each well facilitate lateral orientation of zebrafish larvae following a brief, gentle centrifugation. Reprinted from Lubin et al. [28] under CC-BY license. C) Stamps for creating troughs in agarose within multi-well plates for larvae alignment. (i) Photograph of a 3D printed tool used to create troughs for zebrafish larva orientation in agarose within 96-well plates; reprinted from Wittbrodt et al. [37] under CC-BY license. (ii) Single well illustration of a zebrafish larva oriented vertically by a trough formed in agarose by a tool like the one in (C.i); reprinted from Westhoff et al. [36] under CC-BY license. D) Orientation of zebrafish larvae by microfluidics. Image reproduced from Lin et al. [45] with the permission of AIP Publishing. Top, illustration of a microfluidic device that simultaneously immobilizes dozens of live and awake 7dpf zebrafish larvae, along with the tubing going into and out of the device. Bottom, channels within separate chips are designed to permit visualization of tail motion (green), or preferential lateral (red) or dorsal (blue) orientation. Example images show zebrafish larvae immobilized within each channel type.

plates available from a commercial supplier, and a stamp created and used in the lab to form troughs in agarose that orient the larvae.

Hashimoto plates. 96-well plates fabricated by Hashimoto (Tokyo, Japan) [34] and distributed globally facilitate side-orientation of zebrafish in a fast and efficient manner. Angled walls inside each well slope downward towards the center, as diagramed in Figure 3B. This steep slope design helps orient the zebrafish larvae on their side and facilitate them sliding down to the bottom of the well. At the bottom is a rectangular viewing window spanning the width of the well. As described by Lubin et al. [28], anesthetized fish embryos between 2–4 dpf are simply pipetted into each well with one fish per well. Once all wells are loaded, the plate is gently centrifuged for about 10 seconds then it is ready for microscopy either on an automated high-content imaging microscope, or any standard microscope with a microplate adapter. Embryos align properly within the viewing window and oriented on their side most of the time (>90%) [28].

The novel plate construction allows for fast, easy, and robust orientation of fish embryos on their side. While care must be taken not to damage the fish during pipetting, the fish are visualized while alive and can be rescued from the wells of the plate. The Hashimoto plates support use of high-magnification objectives since the glass bottom corresponds to No. 1.5 cover glass thickness. The plate is limited to a side orientation only, and the price per plate should be taken into consideration. Though the time savings endowed on studies accepting or requiring this orientation is tremendous, since no manual adjustment is required following centrifugation.

Agarose stamp. A more do-it-yourself approach involves creation of a stamp to create a trough within agarose to hold the zebrafish embryos in desired dorsal or on-side orientations. The stamps can be fabricated from polydimethylsiloxane (PDMS) [35], brass [36], or using 3D printing [37]. In each of these cases, the stamp creates a reproducible array of troughs in agarose, often within a 96-well plate. Figure 3C shows an example of a 3D printed tool, along with the alignment troughs it creates.

For fish on their side, a 3D printed stamp also allowed for creation of a slight ‘bump’ having a height approximately equal to the height of the yolk sac and upon which only the tail of the embryo rests [38]. The benefit from such a bump is that the anteroposterior plane of the fish is lying approximately parallel to the focal plane of a microscope objective, thereby optimizing Z-stack image acquisitions.

In all cases, zebrafish embryos are pipetted into the well containing the trough or bump and aligned manually using a pipet tip. The advantage of such stamps is that they are cheap and easy to implement, since they can be created in any lab having a 3D printer and are adaptable

to any microscope. Moreover, the stamps are not limited to a specific model organism or orientation and trough form can be designed to fit specifications for fish other than zebrafish embryos. Though the stamp-and-trough method benefits from reproducible orientation for imaging, the required manual adjustment bottleneck results in a substantial lack of attainable throughput.

Capillary tube orientation – VAST. The current state-of-the art for flexible and automated or semi-automated orientation of zebrafish larvae for microscopy is the VAST BioImager platform (Vertebrate Automated Screening Technology) from Union Biometrica. The technology developed at MIT by Pardo-Martin et al. [39,40] relies on use of a capillary tube to hold, manipulate, and rotate a zebrafish embryo for digital imaging in brightfield. In the simplest configuration, computer-controlled fluidics load the embryos loaded into the capillary tube from a 50 mL stirred conical tube. Control software detects when the fluidics positions a fish in front of the digital camera, then a user defines the desired orientation for still or video image acquisition. For each larva, the software acquires images during a full 360-degree rotation of the capillary tube to calculate the correct rotation angle using correlations with age-matched templates [40]. Acquisition can be one larva at a time with only the loading occurring automatically, or multiple larvae sequentially and automatically with the software detecting the desired orientation.

The VAST system optionally includes add-on modules to load larvae from multi-well plates to enhance throughput of the system, with the option of returning them to the plate after imaging. Separately, users can optionally equip a flow-through pipettor for manual aspiration of larvae. Other add-on modules permit coupling the VAST system to an upright or stereo microscope for higher magnification and fluorescence imaging capabilities. Zhang et al. [41] recently described another example of larva aspiration and orientation within capillary tubes. Specifically, they aimed to overcome issues with aggregation of two or more larvae, immobilization of different aged larvae using a tapered capillary tube without damaging them and increasing the speed of rotation angle detection. They achieved aspiration of single larva from aggregates with 93% efficacy, obtained 100% survival and 3.2 second angle detection time.

While the time saving advantages of the automation provided are clear and have permitted high-throughput 3D tomographic images of whole larvae [42], it is not a complete solution. Lack of accompanying image analysis software thereby necessitates bespoke analysis solution through ImageJ, Python, MATLAB, etc. For 3D visualization, additional software such as ParaView, Imaris or similar are also needed. And the modularity of the system makes it potentially price-prohibitive for many groups or imaging facilities. Maximizing system functionality requires labs or facilities to invest both in the system and human resources to ensure internal software support.

An exciting example of such bespoke implementation for screening with zebrafish is by Dyballa et al. [43]. Their bespoke image analysis solution to extract multiple cardiovascular parameters from images of live, beating hearts inside the larvae, combined with the VAST system to enable high-throughput, is the CardioTox product available for toxicity screening from ZeClinics (www.zeclinics.com). The promise held by such approaches is evident, as CardioTox was recently spun-out into the separate pharmaceutical drug company ZeCardio (www.zecardiotherapeutics.com).

Microfluidics. Microfluidic approaches to zebrafish embryo and larvae manipulation are the subject of a recent and thorough review by Khalili and Rezai [44], and readers are invited to see their publication for specific details. The authors describe several microfluidic chips that can permit investigation of zebrafish behavior and neurobiology without the need for manual manipulation.

Of relevance here, two separate groups developed microfluidic entrapment methods to relying on hydrodynamic forces to trap *live and awake* zebrafish larvae without the need for anesthetic or agarose/gel for immobilization [45,46]. By adjusting the design of the chamber holding the larvae, as depicted in Figure 3D, authors could reliably orient zebrafish either laterally, on their side, or dorsally for neuron visualization to visualize the fully awake animals. The designs are medium throughput, permitting trapping of tens of zebrafish simultaneously.

Of particular importance, microfluidic chips are economical to fabricate once they are designed, potentially lessening the price barrier for adoption. They are also compatible with many types of microscopes, including inverted microscopes and stereo microscopes due to the transparency of many types of microfluidic chips. The bottom of microfluidic chips can be glass coverslips needed to perform high-resolution microscopy using high-magnification objectives, including water, silicon, or oil immersion. Currently, the technology is in its infancy, not being commercially available at the time of this writing, but has great potential for automated, gentle embryo handling.

Image Acquisition

Once a researcher or microscopist has treated, prepared, and oriented a sample of zebrafish embryos, they acquire digital micrographs. Common magnifications are 2x or 4x for imaging a whole zebrafish embryo [28,35], depending on the size of the detection area of the microscope camera, or 10x to 20x for higher resolution images [35,47]. The sample is commonly moved to image multiple fish, either by hand in the case of stereomicroscopes and simple upright or inverted microscopes, or through translation of the microscope stage. It is important to maintain the orientation of the zebrafish embryo during sample movement, which entails gentle movements that avoid jostling or vibrational perturbations. Automated HCS microscopes typically move the sample through stage movement using stepper or piezo motors. Though some HCS microscopes, such as the WiScan Hermes from IDEA Bio-Medical, are different in that the objective is the mobile element, and the sample remains stationary. As such, the sensitivity and requirement for precise embryo orientation must be considered when selecting the most appropriate microscope for imaging. A noteworthy exception is the VAST BioImager that, as described in the previous section, incorporates a fluidic system to manipulate and orient a zebrafish for imaging following extraction from a 96-well plate.

In terms of experiments involving embryo or larva screening, automated HCS microscopes may be beneficial for faster image acquisition compared with manual imaging. Common HCS sample formats are multi-well plates, commonly in 96- or 384-well format, though plates with fewer wells or 35 mm dishes are also commonplace. Depending on conditions, imaging can take from a few minutes for basic widefield imaging of one or a few Z-planes, to several hours if large confocal Z-stack data sets are needed. Through such technology, experiments and screens can be carried out in a rapid, automated fashion for example in a drug screen, combinations of compounds in multiple concentrations can be tested simultaneously [1]. As well, computer control over the microscope allows for analysis-based feedback during acquisition. Many HCS microscopes support object mapping during imaging, wherein a structure of interest is imaged at low magnification in a first scan, then centered for imaging in a second scan with higher magnification [35,48]. This level of content-based automation provides great time saving benefits.

High-content imaging microscopes are a mature technology resulting from broad adoption over more than two decades in both academic and industrial sectors [49]. Hence, using sample types commonly supported and implemented in traditional screening studies involves fewer hurdles in automating imaging of zebrafish embryos. On the other side, some microfluidic approaches may face additional challenges given the difference in sample size, form factors and the requirement for extensive tubing (see Figure 3D).

Table 1
Summary of Automated Image Analysis Software.

Category	Software	Reference	Brightfield	Fluorescence	Auto-mated	Uses AI/ML*	Preserve Anatomy	Spatial Info	Classify Fish	Fiducial free	Availability
Fluorescence only	Quantifish	54		√	√			√		√	Open-Source
	Pixel Classifier	56		√	√	√				√	Open-Source
	Spot with Rings	51		√	√			√		√	Commercial
Phenotype Classification	Deep Fish	59	√		√	√		√	√	√	Open-Source
	ML Classifiers	57	√		√	√			√	√	Open-Source
	Template Matching	60	√		√					√	Open-Source
Brightfield Only	Fish Inspector	61	√		√		√	√	√		Open-Source
Brightfield with Fluorescence	Athena-Zebrafish	28	√	√	√	√	√	√	√	√	Commercial

* AI – Artificial Intelligence; ML – Machine Learning

Image Analysis

Extracting meaningful and quantitative information from digital microscopy images of zebrafish embryos and larvae is a major workflow bottleneck. While the zebrafish model itself provides rich anatomical information, getting a computer to recognize that data is challenging. Zebrafish screens often utilize fluorescence, for example by using a transgenic zebrafish line with the gene or cell of interest tagged with a fluorescent marker, or the injection of fluorescently labelled material. Fluorescence-only image analysis approaches typically do not identify the fish itself, rather only the fluorescence intensity or identifiable spots. Large signal-to-noise makes this a simple choice regarding image analysis but is prone to detection of artefacts from auto-fluorescence or other issues. Moreover, it loses all the non-fluorescent anatomical information visible to the human observer. Brightfield images are more complicated to work with due to broad range of grey intensity values present within images of fish. Computers need sophisticated image analysis to identify structures, though advances in artificial intelligence (AI) are quickly making headway on this front. Few approaches currently combine brightfield and fluorescence detections, but such advanced analysis will be necessary to rapidly process large numbers of animals. Table 1 summarizes the software solutions described here that enable automated image analysis.

Fluorescence only approaches

General Fluorescence Analysis. Images of fluorescently labeled zebrafish are directly amenable to standard image analysis techniques for fluorescence microscopy. Techniques include intensity thresholding, image smoothing and background subtraction with the intent to identify and segment labeled structures visible in the fluorescence images. Software for such analysis include open-source options such as ImageJ/Fiji and Python, licensed software such as MATLAB and Imaris, and software accompanying imaging equipment such as, MetaXpress/Metamorph from Molecular Devices and Kaleido from Perkin Elmer. Mikut et al. [50] previously reviewed uses of these software packages. Here, we group together analysis approaches that specifically take into consideration that the sample is a zebrafish embryo.

While instances of general fluorescence analysis are too numerous to describe in detail, notable examples of its use for high-content screening of zebrafish include:

- Cell count of labeled myelinating oligodendrocytes for a compound screen promoting growth [47] using home-built ImageJ macros together a custom confocal microscope equipped with a VAST BioImager.
- Measurement of fluorescently labeled cell migration from human tumor xenograft [51] using MetaXpress software from Molecular Devices together with an ImageXpress Micro HCS microscope.
- Cell count of labeled cells in the spinal cord for assessment of oligodendrocyte lineage formation [52] using Kaleido analysis software from PerkinElmer together with an EnSight microplate reader.
- Consumption of fluorescently labeled paramecia for appetite regulation gene and drug screening [53] using a stereo microscope and unspecified, in-house software.

Here, analysis of the fluorescent channels enables identification of internal fish anatomy as primary objects, since they are large, overarching structures visible via fluorescence. Fluorescence in either the same channel [47,52] or different channels [47,51] were used to identify and study the behavior of labeled cells, which are smaller, secondary objects. Figure 4A shows an example reprinted from Early et al. [47] where maximum intensity summation in the green fluorescence channel (iii and iv) first identifies the ventral spinal cord of the larva, indicated as blue dots. The software used it to define the adjacent ventral spinal cord region (v). Finally, the software identifies and counts single EGFP (Enhanced Green Fluorescent Protein)-labeled oligodendrocytes inside the dorsal spinal cord (vi). The authors point out that the simple maximum intensity analysis erroneously double-counts a single cell (green arrow), which is corrected using their bespoke '*processCells*' ImageJ function. Both functions still fail to identify dim cells (orange arrow).

Though the signal in fluorescence channels benefits from having large signal-to-noise, the required use of specific fluorescent labels limits the assay's adaptability. Because one fluorescent color must be assigned for identification of primary organ-objects, it leaves one less option available for visualizing other structures and cell types. Requisite delegation of one channel can be quite limiting in zebrafish, since EGFP/GFP and mCherry are commonly used label of choice in transgenic fish. Moreover, autofluorescence or the presence of labeled cells outside the anatomy of interest may introduce unwanted artefacts, and so should be taken into consideration during data analysis.

Quantifish*: Measures Spatial Distribution of Fluorescent spots.* Published in 2020 by Stirling et al. [54], Quantifish is an open-source, stand-alone analysis software written in Python 3 with a simple user interface. The authors designed it within the context of microinjection of fluorescently labeled bacteria into a 24 hpf zebrafish embryo and the entire fish captured in a single image. Their software analyzes fluorescence images using a simple intensity threshold to identify groups of bright pixels corresponding to clusters of bacterial infection and, thus, the pathological burden within an embryo. Figure 4 schematically depicts output of this analysis with the identified clusters shown as green spots upon a generalized zebrafish larva. Although Quantifish [54] uses standard methods for fluorescence analysis similar to those described in the general fluorescence analysis section, it does not attempt to extract any fish-related structures, even though the metrics output are designed with the input of zebrafish images in mind. Too, its approach is subjected to similar channel limitations and potential for artefacts.

The novel aspect of this software is the variety of metrics that it automatically extracted regarding the spatial distribution of the bacterial clusters not identified in other software (Fig. 4B). Three novel metrics attempt to quantify infection spread. The first is the 'grid-area' containing clusters (Fig. 4B.i), calculated by dividing the fluorescence image into squares of user-specified size and summing the area of all squares

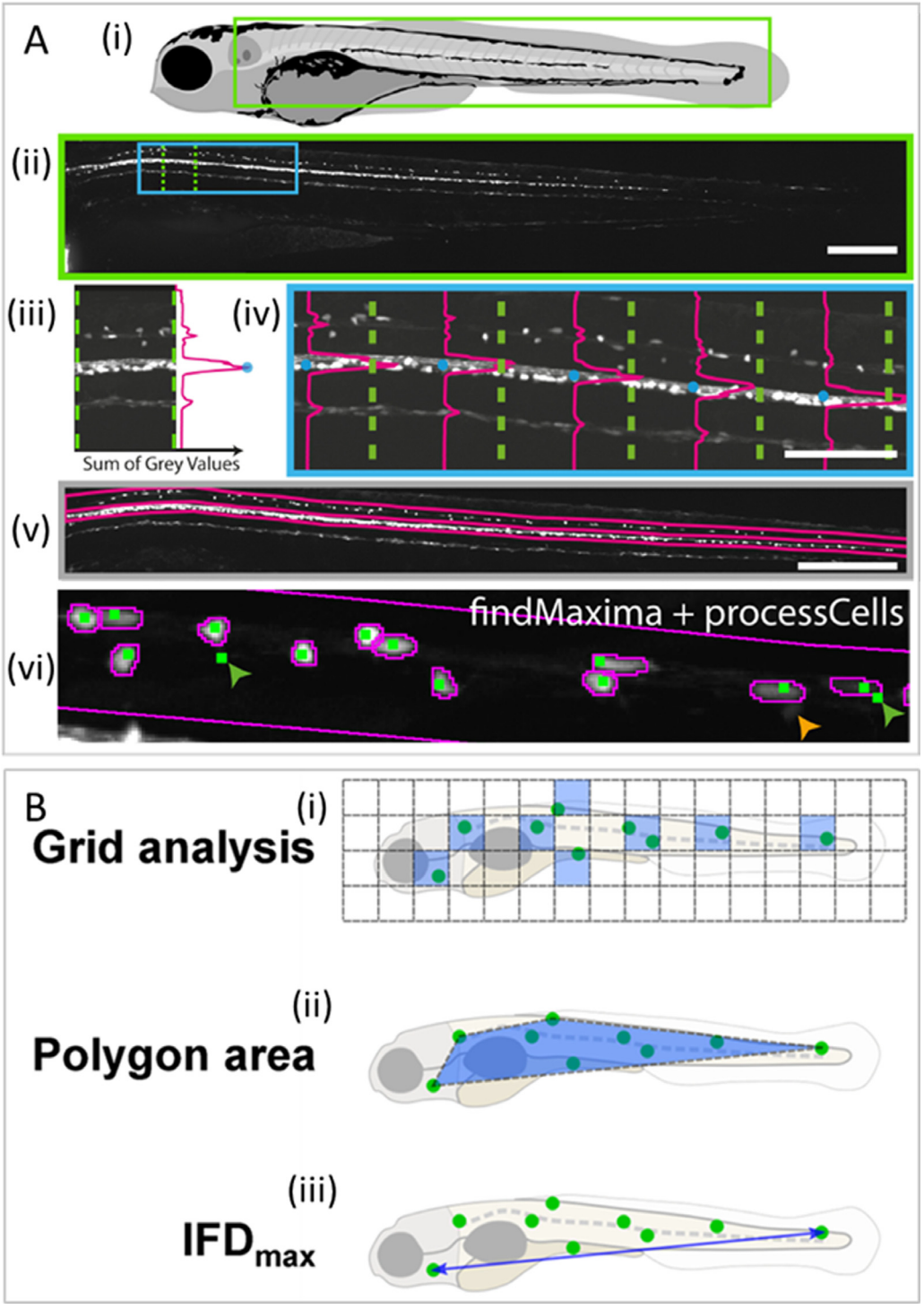

Fig. 4. Fluorescence Image Analysis. A) Identification and segmentation of myelin enriched cells in the ventral spinal cord of 4 dpf zebrafish larvae; reprinted from Early et al. [47] under CC-BY license. (i) Schematic of 4 dpf larva to illustrate the anatomical region shown in subsequent fluorescence images. (ii) Fluorescence confocal image of Tg(mbp:EGFP) within the green rectangle in A.i. (iii) Example of the fluorescence channel snippet within the dashed green lines in A.ii. A vertical profile plot (magenta) of the sum of grey values along the horizontal axis shows how the software identifies labeled anatomy. A blue dot indicates the maximum. (iv) Multiple snippets showing profile plots and indicating that the blue dot follows the bright intensity along the length of the ventral spinal cord. (v) Joining the points delineates the ventral spinal cord in the GFP channel, which the authors used to set regions of interest for the dorsal and ventral spinal cords. (vi) Within the dimmer dorsal spinal cord, the software identified and counted single EGFP-labeled oligodendrocytes, surrounding them with a pink outline for visualization shown here. Green arrow indicates a location where maximum intensity identification double-counts a cell; orange arrow indicates the location of a dim yet visible cell that the software fails to identify. Note: the figures originally published in Early et al. [47] have been adapted for clarity of presentation herein. B) Schematic diagrams showing metrics quantified by the Quantifish software; reprinted from Stirling et al. [54] under CC-BY license. Zebrafish larvae in grey contain green dots that represent fluorescent foci, or clusters, identified by fluorescence image analysis. Quantifish extracts three specialized spatial distribution metrics: (i) Grid analysis: This analysis divides the image into an array of squares, then counts the number of squares containing the centroid of one or more foci (highlighted in blue). (ii) Polygon area: This analysis defines a closed polygon of arbitrary number of vertices that encompasses all foci centroids. (iii) IFDmax: The maximum inter-foci distance (IFD) is the largest distance separating the centroid of any two foci in the image.

containing a cluster. The second is the area of a polygon encapsulating all the clusters (i.e., Convex Hull, Fig. 4B.ii). The third is the largest distance separating a pair of clusters (Fig. 4B.iii). Simple metrics extracted by Quantifish include the total integrated fluorescence intensity, and the count and area of the clusters. Through quantifying this diverse array of metrics, the authors were able to distinguish between intravenous and hindbrain bacterial microinjection routes of infection, which are indistinguishable by simple fluorescence integration and spot counting.

This approach benefits from being open-source and having an easy-to-use interface. Though, the simplicity of the thresholding algorithm makes it susceptible to errors arising from auto-fluorescence, background artefacts or poor signal-to-noise. As well, because the software disregards the zebrafish anatomy of the brightfield images, it cannot place the location of data extracted in relation to distance from the site of microinjection, which may be of potential relevance for the study at hand.

Machine-Learning pixel classifier. Machine learning algorithms offer the ability to readily identify structures and objects in an image through pixel-based classification. The classification can be performed on fluorescence images, for example on fish containing EGFP-labeled vasculature [55], or on RGB images of traditional stains, such as o-dianisidine hemoglobin stain [56]. Multiple machine learning implementations can be used, such as commercial Google AutoML [55] or open-source Ilastik in combination with CellProfiler [56]. In both instances, the software determines and selects pixels containing signal of interest based on how a user trains the underlying algorithm. The output can classify an input image as either 'normal' or 'abnormal' [55], or can select signal-positive pixels and use their intensity information for quantitative comparison [56].

An advantage of machine-learning approaches is the ease of use once trained. Users feed input images into the algorithm and software outputs a result output with no further interaction. Such flexibility of input image type (greyscale, RGB, etc.) allows a variety of specific staining methods to visualize zebrafish.

Such simplicity can be a double-edge sword, as it may be used as a sort of black-box. Users can get results without understanding how the software generates results. For this reason, simple intensity-only measurements may benefit from the use of more straightforward analysis algorithms, such as with Quantifish. Indeed, both approaches potentially suffer from artefactual intensity measurements arising from non-specificity or background artefacts. Lastly, while machine learning can permit object identification and segmentation, the two implementations described here did not attempt to extract such information. As such, the authors did not utilize the morphology of the zebrafish embryo whatsoever, though in principle machine learning could potentially extract anatomical information.

Brightfield imaging approaches

Rapid classification of zebrafish embryos according to their phenotype visualized in brightfield microscopy images can greatly facilitate toxicology and genetic screens. This type of analysis aims to quickly sort individual fish into bins, such as normal, dead, etc. Machine learning, deep-learning and template-matching methodologies are making advances in this front to expedite analysis in an unbiased fashion. Another approach attempts to identify zebrafish larvae and their internal anatomy automatically from brightfield images. While challenging, this type of analysis quantifies numerous morphological metrics ignored by classification-only approaches, and which could still be used for classification.

Phenotype classification. The shape of a zebrafish embryo can be indicative of a healthy or diseased state. While such classification can be rapidly determined by experienced human observers, removing the bias and increasing throughput are highly desirable. Jeanray et al. [57] utilized supervised machine learning utilizing a randomized tree approach, which used raw pixel values as input. They trained their algorithm using 529 annotated images to automatically classify 11 distinct phenotypes: Normal, with Chorion, Down-Curved Tail, Up-Curved Fish, Up-Curved Tail, Up-Curved Tail/Fish, Short Tail, Hemostatic, Necrosed Yolk, Edema and Dead. Images could pertain to only one of the phenotypes and did not permit mixing. Figure 5A reprints six of these phenotypes [57] to highlight the similarity among some of them. Processing time required only 400 ms per image. Though the authors performed image acquisition manually using a stereomicroscope and image preprocessing using an ImageJ macro. As such, their approach can readily scale to a more fully automated implementation.

With a test set of 341 images the authors determined that, depending on the phenotype, it chose the same categorization as three expert researchers between 50-100% of the time. With respect to images shown in Figure 5A, the authors report 90-95% certainty for normal, necrosed yolk sac and up curved fish (panels i, ii and vi, respectively). The up curved tail and short tail (panels iii and iv) phenotypes had 85-89% certainty, but the certainty of hemostasis (panel v) was the lowest of all at only 51% certainty. Upon treatment with eight compounds, the dose-response curves created from the algorithm's categorization agreed well with those obtained from manual analysis, including EC_{50}, LC_{50} and teratogenicity index (TI) values. Subsequent work reported similar results when performing classification using a fine-tuned convolution neural network (CNN) deep-learning approach [58].

Ishaq et al. [59] described a more simplified binary classification using a deep-learning approach and their software is openly available as their 'Deep Fish' software. While their approach aimed only to classify zebrafish embryos as either deformed (bent tail) or normal with a single treatment condition, they were able to achieve accuracy of ~93% with respect to human classification, using only 84 images as training input. Like Jeanray et al. [57], images could only pertain to one classification category. In terms of throughput, their algorithm required only 360 ms to classify 28 test images, representing more than a 30-fold increase in speed.

While phenotype classification is important for rapid screening in terms of general toxicology, it may not be indicative of the underlying cause of deformations or disease state. As well, the classification relies on correlations with large morphological characteristics, but does not extract morphological metrics for quantitative comparisons. As with the fluorescence-based classification algorithms described above, untrained users may use such classification as a black-box only to get an answer without understanding how those underlying groups are determined.

Template matching. Because zebrafish embryos appear similar to one another, they are amenable to template matching (Fig. 5B). In this approach an example image, or cropping of an image, is moved (translated) over a test image to detect its presence is used to identify the presence of a similar object in a test image. The images and template can be brightfield or fluorescence images. Once a template is input, the detection is automatic and can be performed with as little as a single template. A recent implementation by Thomas and Gehrig [60] is openly available on multiple platforms – Fiji/ImageJ, KNIME and Python. Though they demonstrated the utility of template matching using zebrafish embryos, their approach and algorithm is applicable to many other sample types.

In addition, their software allows for input of multiple templates and multiple detections while also removing aberrant overlapping template matches through non-maxima suppression. They demonstrate automated and iterative selection of zebrafish regions (head) and anatomy (eye) (Fig. 5B) through successive template matching. In this context, they first identify the fish embryo itself. Within the fish, the algorithm could identify either the head or the eyes through an appropriate template. Matching to a template requires a user-defined score threshold ranging from 0–1, which the authors varied as they demonstrated their approach. Using a standard desktop computer with the OpenCV library, the authors could perform template matching on a 96-well plate in less than 1.5 seconds, demonstrating a high image throughput.

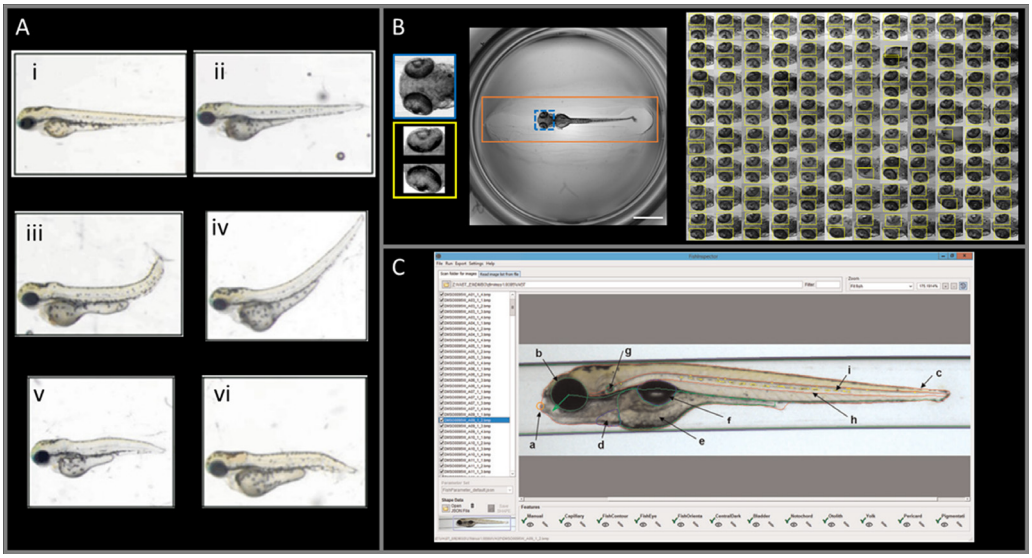

Fig. 5. Brightfield Image Analysis. **A)** Example images of zebrafish larvae phenotypes distinguished by machine learning, reprinted from Jeanray et al. [57] under CC-BY license. The phenotypes shown are: "Normal" (i); "Necrosed Yolk Sac" (ii); "Up Curved Tail" (iii); "Up Curved Fish" (iv); "Short Tail" (v); "Hemostasis" (vi). Note: each image was cropped from the original figure to create the panel shown here. **B)** Template matching for identifying zebrafish larva and internal anatomy. Images reprinted from Thomas and Gehrig [60] under CC-BY license. Left: Templates of the head and eyes used to identify the anatomy within larger images. Center: Image of a 3dpf zebrafish embryo oriented dorsoventrally. The orange rectangle shows an optional search region within the template matching software. The blue dotted rectangle identifies the head-region template used for 2-step template matching. Right: Montage of the eye regions detections (yellow) for the 2-step matching approach across a 96-well plate. Note: the original figure was edited to include the template of the head; the images were slightly realigned. **C)** Screenshot image depicting the FishInspector software graphical user interface and the anatomy it identifies. Image reprinted from Teixido et al. [61] by permission of Oxford University Press on behalf of the Society of Toxicology. Structures identified: a, lower jaw tip (orange); b, eye contour (green); c, fish contour (red); d, pericard (blue); e, yolk sac (green); f, swim bladder (blue); g, otolith (green); h, notochord (green); i, pigmentation (yellow). Note the dark lines from the encapsulating capillary tube visible above and below the larva. These reference structures are a key starting point for the FishInspector software.

The implementation on flexible platforms can permit users to build analysis around the template matching algorithm, thereby permitting measurement of fluorescence information using objects detected in brightfield. However, the authors themselves did not demonstrate such an example. Nor did they demonstrate if their algorithm is adaptable to deviations from a template, such as those observed in phenotypic screens using the classifier approaches described previously (Fig. 5A).

FishInspector*: Larva anatomy segmentation and morphology measurement.* In a similar, yet potentially more powerful, approach to morphological phenotyping for classification is the FishInspector software developed by Teixido et al. [61] (Fig. 5C). The authors designed the software to work with the VAST BioImager for image acquisition. It detects zebrafish embryos in brightfield images and quantifies metrics regarding morphology for use in toxicology and classification. FishInspector is capable of automatically identifying the fish contour, eye, lower jaw tip, pericard, yolk sac, swim bladder, otolith, notochord and pigmentation, while extracting 10 quantitative metrics. Users also have the option to intervene and manually adjust or identify anatomical structures. The authors built the software within the MATLAB environment and intended for data analysis workflows within KNIME and R, which directly receive the coordinates of detected structures without the need for users to do any programming themselves.

The authors demonstrate the ability for unsupervised imaging and analysis, when used with the VAST BioImager, at a rate of three hours per 96-well plate – two hours for acquisition, one for analysis. They also show compatibility with images acquired on a stereomicroscope, potentially making it more broadly usable, but the authors needed to alter images to have a virtual capillary structure surrounding the fish. FishInspector requires this pre-processing because it first detects the capillary border (Fig. 5C), then it subsequently identifies the fish contour and anatomy in a hierarchical order. If it does not identify a structure at the top of the hierarchy, then it cannot identify subsequent structures.

The authors demonstrate the FishInspector's capacity to identify morphological changes in response to compound treatment. They verify EC_{50} calculated using extracted metrics with those obtained using visual inspection of the same images. Of note, the FishInspector data was able to reveal an EC_{50} for treatment with dexamethasone based on several morphological features, while visual assessment did not produce an EC_{50}. A separate, contracted laboratory later verified their result for compound toxicity. Although the authors did not show the capability for multiplexed detection in both brightfield and fluorescence channels, MATLAB has powerful image analysis capabilities that could readily be added to the FishInspector base program. However, for more broad use, the interface should ideally be extended to remove the requirement for capillary edge identification as a starting point.

Combined analysis

Athena-Zebrafish*: Larva anatomy segmentation for combined morphology and fluorescence analysis.* To combine the anatomy visualization in brightfield analysis and fluorescence analysis for cell-type specific labeling, Idea Bio-Medical recently developed new software utilizing AI and demonstrated several use cases for application [28]. A deep-learning CNN algorithm was employed to overcome the difficulty of identifying zebrafish embryos in brightfield. As such, the software does not require user input or external fiduciary marks. The software also identifies fish body regions–head, trunk, and tail–and internal anatomy–eye, otic vesicle, heart, yolk sac, swim bladder, notochord, and tail fin anatomy (Figure 1). The software is an application within the WiScan Athena image analysis platform accompanying the WiScan Hermes HCS microscope used for imaging.

Athena-zebrafish quantifies fish morphology for phenotypic classification, like FishInspector, but also couples to the fluorescence channel(s). Therein, the software identified fluorescently labeled structures and associated them with all relevant anatomy or regions that they fall within. For instance, fluorescent spots identified in the eye of a fish are associated with the fish contour, the head region and eye anatomy. Thus, phenotype classification can focus on specific body regions and thereby exclude fluorescent objects detected in other areas, such as the

yolk which exhibits notable auto-fluorescence when excited with 488 nm light.

To demonstrate the utility of this approach, the Lubin et al. [28] counted numbers of GFP-labeled hematopoietic stem and progenitor cells (HSPC) identified in the caudal hematopoietic tissue (CHT). Manual and automated cell numbers within the fish were in good agreement, were dependent upon the age of the embryos, and showed reduced numbers upon exposure to non-lethal doses of x-ray irradiation. Critical to HSPC counting was the ability to count only those GFP spots present in the tail region where the CHT resides, while ignoring those in other GFP spots or false detections from yolk auto-fluorescence. The authors also performed other spot-based analyses, including acridine orange staining for apoptosis, hair cell staining for ototoxicity screening and a double-color transgenic fish where visualization differentiated myeloid cells from HSPC. Because the software relies on AI, like some classification approaches described previously, brightfield-only analysis identified morphology changes in the eye size in embryos carrying mutations known to cause microphthalmia.

Reliable HSPC counting required an on-side only orientation, achieved through use of the Hashimoto alignment plates described above. Alignment of the fish in the plates required about two minutes of pipetting and no manual adjustment following centrifugation. The software removed improperly aligned fish in post-processing through identification of anatomy: one eye and presence of a tail region. Authors acquired images on a WiScan Hermes microscope using five Z-slices with two colors in about 15 minutes. Image pre-processing required 20 minutes and analysis another 10 minutes, thus permitting acquisition of multiple plates in a day. Though not demonstrated, the combined approach described should be compatible with stamp-based agarose fish orientation techniques, as well as other types of images, such as those from stereomicroscopes, upon appropriate AI training.

Discussion

Incorporation of automation for zebrafish embryo screening not only increases achievable throughput, but also enables more reproducible results and benefits from being traceable. The computer control and digital images, along with analysis settings, leaves a record of every step performed along an experimental workflow. Additionally, researchers can re-visit and re-analyze data to extract different metrics, increasing the data that can be extracted from each sample.

Application of zebrafish to compound toxicology provides examples of automation in some portions of zebrafish manipulation, imaging, and high-content analysis to increase throughput. But some areas still require additional development for a fully automated pipeline. Wlodkowic and Campana [62] review several automated technologies surrounding the fish embryo toxicity test (FET). Originally known as the Acute Fish Toxicity Test (AFT), intended to determine acute chemical toxicity, the FET became an official standardized test in 2013 approved by the Organization for Economic Co-operation and Development (OECD). As such, worldwide acceptance for chemical toxicity testing can include data output from FET studies. Technologies that automate portions of FET include: dechorionation, microperfusion for compound exposure, and imaging. Areas where additional automation requires development includes selection of fertilized eggs through visualization blastomere formation and improvements in image analysis, as described herein.

ZeClinics has commercialized a cardiovascular toxicology test, CardioTox [43], where automation is key to achieving the scalability and reproducibility required of a for-profit endeavor. Their approach utilizes the VAST BioImager system coupled to a widefield, fluorescent microscope equipped with a high-speed camera to acquire images at 70 – 76 frames per second. Their proprietary, semi-automatic ZeCardio software analyzes video data to extract a range of metrics related to the heart morphology and function while it is beating. In their initial study, the authors performed a cross-comparison of data from different sources to demonstrate that use of zebrafish larvae allowed for a more reliable prediction for cardiotoxic compounds as compared to cell-based toxicology systems.

The existing solutions for automating zebrafish manipulation and imaging workflows are available from a combination of open-source and commercial suppliers. Each solution and source come with its own benefits and drawbacks that researchers will need to evaluate relative to their needs and goals. In Table 2, we compile a few considerations that should be taken into account when evaluating between open-source image analysis options and proprietary solutions from commercial sources. For tinkerers, there are ample opportunities to bring these solutions together in novel fashions and work towards a more streamlined screening workflow (Figure 2).

Towards Fully Automated Workflows

It is an exciting time right now for the prospect of whole organism, in vivo screening using zebrafish. Given the growing popularity of zebrafish as a model organism, the coming years will no doubt see creative re-workings of the first attempt technologies described here, with novel integrations joining them together. It is unlikely that one, single dominant design emerges given the flexibility of the zebrafish for study. Overall, technology for automating microscopic imaging of zebrafish, and analyzing those images, exists and is well developed with several options available. Automating sample preparation, however, provides more opportunity for novel development, as suggested schematically in Figure 2.

Coupling existing solutions through collaboration or commercial partnerships is a likely first step forward. For instance, merging the deep-learning powered microinjection approach [31] with the automated zebrafish embryo dechorionation processes [29] could be a common first-step in many genetic, toxicology and compound screens. Microinjection may be the first step since the chorion is easily pierced during this process. Removal of the chorion and selection of live, undamaged embryos for placement into designated chambers opens ample flexibility for downstream measurement.

For workflows aiming for maximizing throughput, approaches incorporating multi-well plates are the platforms poised to have the fastest adoption. Moreover, multiple liquid handing options exist for dispensing into such plates. Researchers with access to automated HCS microscopes for imaging can readily adopt fast, manual-free options such as the Hashimoto plate [34]. Development of automated dispensing of embryos into wells having an alignment cavity created by a stamp would allow increased flexibility regarding fish orientation, being either on its side or back. Capillary-based approaches are already an enabling technology permitting high-content screens on zebrafish larvae but are still comparatively slow in overall per-fish processing time as compared to traditional HCS benchmark times. Challenges here rely on the automated orientation of the zebrafish embryos required for many types of imaging.

Microfluidics-based approaches are more nascent and those offering fish orientation selection currently have lower throughput, being in the 10s of fish, but benefit from being amenable to awake fish. While use of tricaine anesthetic is common, there are obvious advantages to removing it from experimental setups, particularly when studying compound toxicity. Combining microfluidic approaches with AI to automate sorting and selection of zebrafish embryos or larvae might replace sample manipulation steps that researchers currently perform manually. An advantage, too, of microfluidic approaches is their amenability to microscopy, since a variety of microscopes, and increasingly automated HCS microscope platforms, can readily image the devices. Scalability of chip production and a steep learning curve for adoption and utilization of required pumps and control software by non-expert labs are substantial challenges.

In both instances, use of software incorporated with HCS microscopes or bespoke options built upon existing software can overcome image analysis bottlenecks, such as those described in Table 1. An inter-

Table 2
Comparison of Open-Source vs. Proprietary Automation Solutions.

Consideration	Open-Source	Commercial Supplier
Uniformity	• In-house fabrication can have larger variation before expertise is gained, which can impact samples and data quality. • Source code is available but may be modified by different groups for their needs and not shared with the community, since doing so requires substantial expertise. • Trained AI algorithm may not necessarily be part of source code, rather trained in-house.	• Source code is closed, but well maintained and consistent; different versions are documented and closely monitored. • Trained AI algorithm is uniformly distributed to all users, particularly if the algorithm takes advantage of cloud storage and computing.
Comparability across labs	• Objects identified by Machine Learning and Deep Learning depend on the data input as a training set; differing training sets can lead to different results. • Large, broad and diverse image data sets are needed to ensure a robust AI detection algorithm but are not yet existent.	• In-house AI training by the company ensures a consistent product in each lab using the product. • Benefits from a network effect where the diversity of users permits robust training of the underlying AI to meet the needs of all of them.
Adaptability	• Highly adaptable – existing solutions can be extended and are amenable to de novo creation of bespoke algorithms, macros, scripts, etc. • Higher entry barrier to obtain and, ideally, retain programming and analysis knowledge within a lab.	• Supplier-dependent, with some providers of software being more willing and open to perform custom development in collaboration with labs. • Development timelines depend on the priority determined within private suppliers to adapting their software.
Technical Support and User Interface	• Lab-dependent. Some labs are dedicated to algorithm development, maintenance and dissemination through ImageJ/Fiji, Git Hub and other openly accessible platforms. • Expertise in particular software may readily be lost when a PhD or Postdoc fellowship ends. • User interface is dependent upon the developer and the lab; can be GUI or command-line driven.	• Reliable, expert technical support and updates are commonly available as long as the company exists and supports the product. • Technical support and user interface packages are company dependent and poor service from a 3rd party can substantially hinder research progress.
Cost	• No direct cost barrier regarding access to software. • Potential indirect costs for time to learn new software can be substantial if the lab has no existing expertise and/or the desired software is not created in a user-friendly fashion. • Labs without technical expertise with programming may be locked out of the do-it-yourself option.	• High direct cost barrier involving upfront costs and, frequently, periodic subscription or maintenance costs. • Current technology is still modular with no unified pipeline available, with large investment being required for each piece. • Low indirect cost due to presence of on-demand technical support to ensure proper usage (will vary by company dedication to customer relations).

esting possibility would be to combine zebrafish larvae immobilization for high-content visualization with subsequent release for behavioral observation within a single chip or platform. The potential ability to obtain correlative information between microscopically visible phenotype and behavior is certainly an advantage of the zebrafish model.

In summary, many options are on the table regarding tools available to zebrafish researchers aiming to perform screening on zebrafish embryos and larvae. The challenge ahead is creation of the 'glue' to bring these developments together into a single, streamlined platform.

Declaration of Interest

Authors J.J.O. and Y.P. are currently employed by IDEA Bio-Medical.

Acknowledgments

A.L. and E.M.P. are funded by the CRUK advanced clinician scientist fellowship to Elspeth M. Payne – Grant number A24873.

References

[1] Pegoraro G, Misteli T. High-Throughput Imaging for the Discovery of Cellular Mechanisms of Disease. Trends Genet 2017;33(9):604–15.
[2] Guzi TJ, Paruch K, Dwyer MP, et al. Targeting the Replication Checkpoint Using SCH 900776, a Potent and Functionally Selective CHK1 Inhibitor Identified via High Content Screening. Mol. Cancer Ther. 2011;10(4):591–602.
[3] Danovi D, Folarin A, Gogolok S, et al. A High-Content Small Molecule Screen Identifies Sensitivity of Glioblastoma Stem Cells to Inhibition of Polo-Like Kinase 1. PLoS One 2013;8(10):e77053.
[4] Brodin P, Christophe T. High-content screening in infectious diseases. Curr Opin Chem Biol 2011;15(4):534–9.
[5] Nichols A. High content screening as a screening tool in drug discovery. Methods Mol Biol 2007;356:379–87.
[6] Lin S, Schorpp K, Rothenaigner I, et al. Image-based high-content screening in drug discovery. Drug Discov Today 2020;25(8):1348–61.
[7] Langhans SA. Three-Dimensional in Vitro Cell Culture Models in Drug Discovery and Drug Repositioning. Front. Pharmacol. 2018;9:6.
[8] Seyhan AA. Lost in Translation: the Valley of Death Across Preclinical and Clinical Divide – Identification of Problems and Overcoming Obstacles. Transl. Med. Commun. 2019;4(18).
[9] Giacomotto J, Ségalat L. High-Throughput Screening and Small Animal Models, Where Are We? Br. J. Pharmacol. 2010;160(2):204–16.
[10] Singh S, Carpenter AE, Genovesio A. Increasing the Content of High-Content Screening: An Overview. J. Biomol. Screen. 2014;19(5):640–50.
[11] Boutros M, Heigwer F, Laufer C. Microscopy-Based High-Content Screening. Cell 2015;163(6):1314–25.
[12] Kriston-Vizi J, Flotow H. Getting the Whole Picture: High Content Screening Using Three-Dimensional Cellular Model Systems and Whole Animal Assays. Cytometry A 2017;91(2):152–9.
[13] Booij TH, Price LS, Danen EHJ. 3D Cell-Based Assays for Drug Screens: Challenges in Imaging, Image Analysis, and High-Content Analysis. SLAS Discovery 2019;24(6):615–27.
[14] Faure E, Savy T, Rizzi B, et al. A Workflow to Process 3D+Time Microscopy Images of Developing Organisms and Reconstruct Their cell Lineage. Nat. Commun. 2016;8674:7.
[15] Lessman CA. The Developing Zebrafish (Danio rerio): A Vertebrate Model for High-Throughput Screening of Chemical Libraries. Birth Defects Res. C Embryo Today. 2011;93(3):268–80.
[16] Gehrig J, Pandey G, Westhoff JH. Zebrafish as a Model for Drug Screening in Genetic Kidney Diseases. Front. Pediatr. 2018;6:183.
[17] Li S, Xia M. Review of high-content screening applications in toxicology. Arch. Toxicol. 2019;93(12):3387–96.
[18] Westerfield M. The Zebrafish Book. A Guide for the Laboratory Use of Zebrafish (Danio rerio). 4th ed. Eugene: University of Oregon Press; 2000.
[19] Kimmel CB, Ballard WW, Kimmel SR, et al. Stages of Embryonic Development of the Zebrafish. Dev Dyn 1995;203:253–310.
[20] Parichy DM, Elizondo MR, Mills MG, et al. Normal Table of Post-Embryonic Zebrafish Development: Staging by Externally Visible Anatomy of the Living Fish. Dev Dyn 2009;238(12):2975–3015.
[21] Howe K, Clark M, Torroja C, et al. The Zebrafish Reference Genome Sequence and its Relationship to the Human Genome. Nature 2013;496:498–503.
[22] Phillips JB, Westerfield M. Chapter 47 - Zebrafish as a Model to Understand Human Genetic Diseases. In: Cartner SC, Eisen JS, Farmer SC, Guillemin KJ, Kent ML, Sanders GE, editors. The Zebrafish in Biomedical Research. Academic Press; 2020. p. 619–26.

[23] Rebelo de Almeida C, Mendes RV, Pezzarossa A, et al. Zebrafish Xenografts as a Fast Screening Platform for Bevacizumab Cancer Therapy. Commun. Biol. 2020;3(1):299.
[24] Patton EE, Zon LI, Langenau DM. Zebrafish Disease Models in Drug Discovery: from Preclinical Modelling to Clinical Trials. Nat. Rev. Drug Discov. 2021;20(8):611–28.
[25] Hwang W, Fu Y, Reyon D, et al. Efficient Genome Editing in Zebrafish Using a CRISPR-Cas System. Nat. Biotechnol. 2013;31(3):227–9.
[26] Lin HF, Traver D, Zhu H, et al. Analysis of Thrombocyte Development in CD41-GFP Transgenic Zebrafish. Blood 2005;106(12):3803–10.
[27] Buchan KD, Prajsnar TK, Ogryzko NV, et al. A Transgenic Zebrafish Line for In Vivo Visualisation of Neutrophil Myeloperoxidase. PLoS One 2019;14(4):e0215592.
[28] Lubin A, Otterstrom JJ, Hoade Y, et al. A Versatile Automated High-Throughput Drug Screening Platform for Zebrafish Embryos. Biology Open 2021 in press.
[29] Mandrell D, Truong L, Jephson C, et al. Automated Zebrafish Chorion Removal and Single Embryo Placement: Optimizing Throughput of Zebrafish Developmental Toxicity Screens. J Lab Autom 2012;17(1):66–71.
[30] Henn K, Braunbeck T. Dechorionation as a Tool to Improve the Fish Embryo Toxicity Test (FET) with the Zebrafish (Danio rerio). Comp. Biochem. Physiol. C Toxicol. Pharmacol. 2010;153(1):91–8.
[31] Cordero-Maldonado ML, Perathoner S, van der Kolk KJ, et al. Deep Learning Image Recognition Enables Efficient Genome Editing in Zebrafish by Automated Injections. PLoS ONE 2019;14(1):e0202377.
[32] Carvalho R, de Sonneville J, Stockhammer OW, et al. A High-Throughput Screen for Tuberculosis Progression. PLoS ONE 2011;6(2):e16779.
[33] Spaink HP, Cui C, Wiweger MI, et al. Robotic Injection of Zebrafish Embryos for High-Throughput Screening in Disease Models. Methods 2013;62:246–54.
[34] Hashimoto Z.F.Plate. https://www.funakoshi.co.jp/exports_contents/80394 (accessed May 31, 2021).
[35] Peravali R, Gehrig J, Giselbrecht S, et al. Automated Feature Detection and Imaging for High-Resolution Screening of Zebrafish Embryos. BioTechniques 2011;50(5):319–24.
[36] Westhoff JH, Giselbrecht S, Schmidts M, et al. Development of an Automated Imaging Pipeline for the Analysis of the Zebrafish Larval Kidney. PLoS ONE 2013;8(12):e82137.
[37] Wittbrodt JN, Liebel U, Gehrig J. Generation of Orientation Tools for Automated Zebrafish Screening Assays Using Desktop 3D Printing. BMC Biotechnology 2014;14(36):1–6.
[38] Kleinhans DS, Lecaudey V. Standardized Mounting Method of (Zebrafish) Embryos Using a 3D-Printed Stamp for High-Content, Semi-Automated Confocal Imaging. BMC Biotechnology 2019;19(68):1–10.
[39] Pardo-Martin C, Chang TY, Koo BK, et al. High-Throughput in vivo Vertebrate Screening. Mature Methods 2010;7(8):634–6.
[40] Chang TY, Pardo-Martin C, Allalou A, et al. Fully Automated Cellular-Resolution Vertebrate Screening Platform with Parallel Animal Processing. Lab Chip 2012;12(4):711–16.
[41] Zhang G, Yu X, Huang G, et al. An improved automated zebrafish larva high-throughput imaging system. Computers in Biology and Medicine 2021:136.
[42] Pardo-Martin C, Allalou A, Medina J, et al. High-Throughput Hyperdimensional Vertebrate Phenotyping. Nature Communications 2013;4:1467.
[43] Dyballa S, Minana R, Rubio-Brotons M, et al. Comparison of Zebrafish Larvae and hiPSC Cardiomyocytes for Predicting Drug-Induced Cardiotoxicity in Humans. Society of Toxicology 2019;171(2):283–95.
[44] Khalili A, Rezai P. Microfluidic Devices for Embryonic and Larval Zebrafish Studies. Briefings in Functional Genomics 2019;18(6):419–32.
[45] Lin X, Li VWT, Chen S, et al. Autonomous System for Cross-Organ Investigation of Ethanol-Induced Acute Response in Behaving Larval Zebrafish. Biomicrofluidics 2016;10:024123.
[46] Fuad NM, Kaslin J, Wlodkowic D. Lab-On-A-Chip Imaging Micro-Echocardiography ($i\mu$EC) for Rapid Assessment of Cardiovascular Activity in Zebrafish Larvae. Sens. Actuators B 2018;256:1131–41.
[47] Early JJ, Marshall-Phelps KLH, Williamson JM, et al. An Automated High-Resolution in vivo Screen in Zebrafish to Identify Chemical Regulators of Myelination. eLife 2018;7:e35136.
[48] Booth BW, McParland C, Beattie K, et al. OpenHiCAMM: High-Content Screening Software for Complex Microscope Imaging Workflows. iScience 2018;2:136–40.
[49] Taylor DL. A Personal Perspective on High-Content Screening (HCS): From the Beginning. J. Biomol. Screen. 2010;15(7):720–5.
[50] Mikut R, Dickmeis T, Driever W, et al. Automated Processing of Zebrafish Imaging Data: A Survey. Zebrafish 2013;10(3):401–21.
[51] Zhang B, Shimada Y, Kuroyanagi J, et al. Quantitative Phenotyping-Based In Vivo Chemical Screening in a Zebrafish Model of Leukemia Stem Cell Xenotransplantation. PLoS ONE 2014;9(1):e85439.
[52] Buckley CE, Marguerie A, Roach AG, et al. Drug Reprofiling Using Zebrafish Identifies Novel Compounds with Potential Pro-Myelination Effects. Neuropharmacology 2010;59(3):149–59.
[53] Shimada Y, Hirano M, Nishimura Y, et al. A High-Throughput Fluorescence-Based Assay System for Appetite-Regulating Gene and Drug Screening. PLoS ONE 2012;7(12):e52549.
[54] Stirling DR, Suleyman O, Gil E, et al. Analysis Tools to Quantify Dissemination of Pathology in Zebrafish Larvae. Scientific Reports 2020:10.
[55] Sawaki R, Sato D, Nakayama H, et al. ZF-AutoML: An Easy Machine-Learning-Based Method to Detect Anomalies in Fluorescent-Labelled Zebrafish. Inventions 2019;4(4):72.
[56] Metelo AM, Noonan HR, Li X, et al. Pharmacological HIF2α Inhibition Improves VHL Disease–Associated Phenotypes in Zebrafish Model. Journal of Clinical Investigation 2015;125(5):1987–97.
[57] Jeanray N, Marée R, Pruvot B, Wehenkel L, Muler M. Phenotype Classification of Zebrafish Embryos by Supervised Learning. PLoS ONE 2015;10(1):e0116989.
[58] Tyagi G, Patel N, Sethi I. A Fine-Tuned Convolution Neural Network Based Approach For Phenotype Classification Of Zebrafish Embryo. Procedia Computer Science 2018;126:1138–44.
[59] Ishaq O, Sadanandan SK, Wählby C. Deep Fish: Deep Learning-Based Classification of Zebrafish Deformation for High-Throughput Screening. SLAS Discovery 2017;22(1):102–7.
[60] Thomas LSV, Gehrig J. Multi-Template Matching: A Versatile Tool for Object-Localization in Microscopy Images. BMC Bioinformatics 2020:21.
[61] Teixidó E, Kießling TR, Krupp E, et al. Automated Morphological Feature Assessment for Zebrafish Embryo Developmental Toxicity Screens. Toxicol. Sci. 2019;167(2):438–49.
[62] Wlodkowic D, Campana O. Toward High-Throughput Fish Embryo Toxicity Tests in Aquatic Toxicology. Environ. Sci. Technol. 2021;55(6):3505–13.